Efficient generation of energetic ions in multi-ion plasmas by radio-frequency heating

Kazakov, Ye. O.

Kazakov , Y O , Alcator C-Mod Team , JET Contributors , Ahlgren , T J , Aho-Mantila , L , Airila , M , Asunta , O , Björkas , C M I , Groth , M , Hakola , A , Järvinen , A , Karhunen , J , Koivuranta , S , Lahtinen , A A , Lasa Esquisabel , A , Nordlund , K H & Safi , E 2017 , ' Efficient generation of energetic ions in multi-ion plasmas by radio-frequency heating ' , Nature Physics , vol. 13 , no. 10 , pp. 973-978 . https://doi.org/10.1038/NPHYS4167

Efficient generation of energetic ions in multi-ion plasmas by radio-frequency heating

Ye. O. Kazakov[1]*, J. Ongena[1], J. C. Wright[2], S. J. Wukitch[2], E. Lerche[1,3], M. J. Mantsinen[4,5], D. Van Eester[1], T. Craciunescu[6], V. G. Kiptily[3], Y. Lin[2], M. Nocente[7,8], F. Nabais[9], M. F. F. Nave[9], Y. Baranov[3], J. Bielecki[10], R. Bilato[11], V. Bobkov[11], K. Crombé[1,12], A. Czarnecka[13], J. M. Faustin[14], R. Felton[3], M. Fitzgerald[3], D. Gallart[4], L. Giacomelli[8], T. Golfinopoulos[2], A. E. Hubbard[2], Ph. Jacquet[3], T. Johnson[15], M. Lennholm[16,17], T. Loarer[18], M. Porkolab[2], S. E. Sharapov[3], D. Valcarcel[3], M. Van Schoor[1], H. Weisen[14], JET Contributors[†] and the Alcator C-Mod Team[†]

We describe a new technique for the efficient generation of high-energy ions with electromagnetic ion cyclotron waves in multi-ion plasmas. The discussed 'three-ion' scenarios are especially suited for strong wave absorption by a very low number of resonant ions. To observe this effect, the plasma composition has to be properly adjusted, as prescribed by theory. We demonstrate the potential of the method on the world-largest plasma magnetic confinement device, JET (Joint European Torus, Culham, UK), and the high-magnetic-field tokamak Alcator C-Mod (Cambridge, USA). The obtained results demonstrate efficient acceleration of ^{3}He ions to high energies in dedicated hydrogen–deuterium mixtures. Simultaneously, effective plasma heating is observed, as a result of the slowing-down of the fast ^{3}He ions. The developed technique is not only limited to laboratory plasmas, but can also be applied to explain observations of energetic ions in space-plasma environments, in particular, ^{3}He-rich solar flares.

In magnetized plasmas, charged particles gyrate around the magnetic field lines with their characteristic cyclotron frequencies $\omega_{cs} = q_s B / m_s$, where q_s is the particle's charge, m_s is the particle's mass, and B is the local magnitude of the magnetic field. A variety of strong wave–particle interactions is possible when the wave frequency is close to the particle's cyclotron frequency or its harmonics[1–3]. Ion cyclotron resonance heating (ICRH) is a powerful tool used in toroidal magnetic fusion research. In recent decades, several efficient ICRH scenarios were identified theoretically and verified experimentally[2–4]. In brief, this technique relies on external excitation of fast magnetosonic waves in the plasma, using specially designed ICRH antennas located at the edge of the device (see Fig. 1a). Antennas consist of a series of metallic straps that carry radio-frequency (RF) currents at a given frequency delivered by an external generator. The radially varying toroidal magnetic field then determines the location of the ion cyclotron layers $\omega = p\omega_{ci}$ ($p = 1, 2, \ldots$), in the vicinity of which the RF power can be efficiently absorbed by ions.

The electric field of the excited fast waves can be decomposed as a sum of the left-hand polarized component E_+, rotating in the sense of ions, and the oppositely rotating right-hand component E_-.

Wave absorption by non-energetic ions is evidently facilitated by the presence of a sufficiently large E_+ near the ion cyclotron resonance. To illustrate this, we note that fundamental cyclotron heating in single-ion plasmas is ineffective since E_+ almost vanishes at $\omega \approx \omega_{ci}$.

The choice of plasma composition, namely the number of ion species and their relative concentrations, allows one to control the radial dependence of the ratio E_+/E_-. In two-ion plasmas composed of one main ion species and a few per cent of minority ions with q_i/m_i different from that for the main ions, RF power absorption at the minority ion cyclotron frequency is strongly enhanced[5,6]. These minority heating scenarios benefit from the enhanced E_+ in the vicinity of the ion–ion hybrid (IIH) cutoff-resonance pair, located close to the minority cyclotron resonance[2]. If the IIH layer is not present in the plasma, as is the case at very low minority concentrations in two-ion plasmas, the RF power absorption by minorities is very limited. On the other hand, at minority concentrations significantly above the optimal value of a few per cent, the IIH pair is located too far away from the minority cyclotron layer, thus further reducing their absorption efficiency. Instead, such plasmas are typically used for localized electron heating through mode conversion (see ref. 7 for more details).
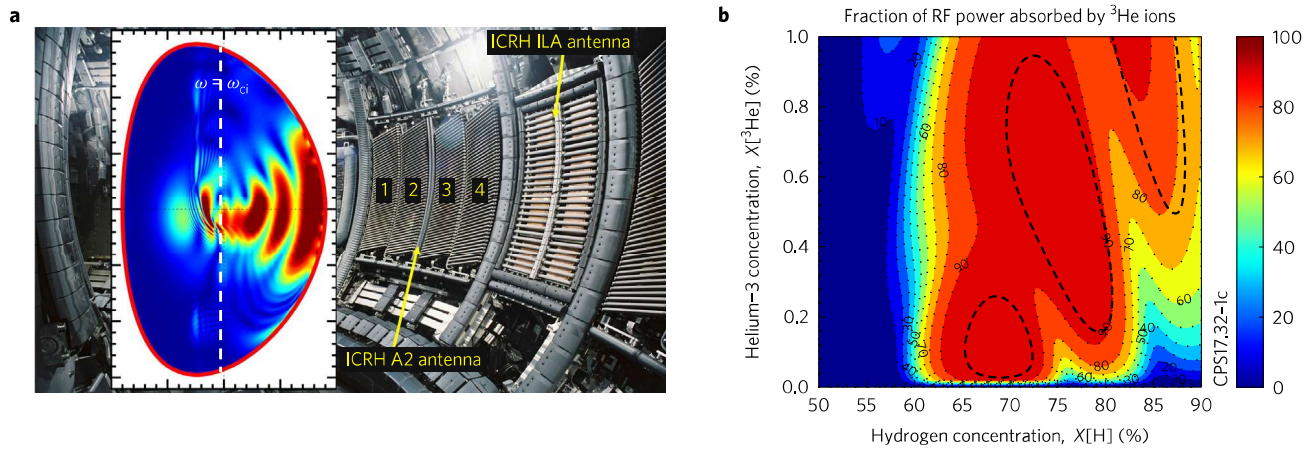
Figure 1 | A new technique for fast-ion generation in magnetized multi-ion plasmas. The goal of our study is to validate that, in properly chosen multi-ion plasmas, electromagnetic ion cyclotron waves can be effectively absorbed by a very low number of resonant ions at $\omega \approx \omega_{ci}$. This technique opens the possibility of high-efficiency generation of energetic ions in magnetized plasmas. **a**, Inside view of the world-largest magnetic confinement fusion device, Joint European Torus, showing different ion cyclotron resonance heating (ICRH) antennas at the edge. The insert shows an example of the computed RF electric field pattern in a cross-section of the JET plasma. **b**, 'Three-ion' scenarios require resonant ions with a (Z/A) ratio in between that of the two main ions, essentially following the 'sandwich' principle $(Z/A)_2 < (Z/A)_3 < (Z/A)_1$. The figure shows the fraction of RF power absorbed by ^{3}He minority ions for the D–(^{3}He)–H three-ion scenario as a function of H and ^{3}He concentrations. The computations were made by the TOMCAT code for the parameters of the JET experiments discussed in this paper ($B_0 = 3.2$ T, $f = 32.5$ MHz, $n_{e0} = 4 \times 10^{19}$ m^{-3}, $T_0 = 4$ keV, $k_{\parallel}^{(ant)} = 3.4$ m^{-1}). The zones within the dashed lines correspond to a single-pass absorption larger than 50%. The code predicts wave absorption by a tiny amount of ^{3}He ions ($\sim$0.1–0.2%) in H–D plasmas with H concentrations in the range 70–80%, in agreement with equation (2).

There is, however, an elegant way to use mixture plasmas to channel RF power to ions: simply add a third ion species with a cyclotron resonance layer close to the IIH cutoff-resonance pair. Under these conditions, a new IIH pair appears in close proximity to the cyclotron resonance of the third ion species, even if their concentration is extremely low! For this heating scheme to work, the Z/A value of the resonant ions should be 'sandwiched' between that of the two main plasma ions

$$(Z/A)_2 < (Z/A)_3 < (Z/A)_1 \qquad (1)$$

where Z_i and A_i are the charge state and the atomic mass of ion species i. We use indices '1' and '2' for the main ions with the largest and lowest cyclotron frequencies, respectively, and index '3' for the absorbing minority. Depositing nearly all RF power to a very small number of minority ions is maximized in plasmas with main ion concentrations[8,9]

$$X_1^* \approx \frac{1}{Z_1}\frac{(Z/A)_1 - (Z/A)_3}{(Z/A)_1 - (Z/A)_2}, \quad X_2^* \approx \frac{1}{Z_2}\frac{(Z/A)_3 - (Z/A)_2}{(Z/A)_1 - (Z/A)_2} \qquad (2)$$

where $X_i = n_i/n_e$. Heating minority ions at higher concentrations is equally possible; plasma mixtures with $X_1 \gtrsim X_1^*$ are more optimal in this case[10]. The method can also be extended to plasmas containing more than three ion species by slightly adapting the plasma composition. For proof-of-principle demonstration, we select a plasma mixture composed of two hydrogen isotopes, H ions with $(Z/A) = 1$ and the heavier D ions with $(Z/A) = 1/2$, and ^{3}He ions with their unique $(Z/A) = 2/3$ as a resonant absorber. Equation (2) predicts that ^{3}He ions should efficiently absorb RF power in H–D (or H–^{4}He) plasmas if the hydrogen concentration is $\sim$67%. This is supported by modelling with the TOMCAT code[11], using plasma parameters relevant for the JET experiments described below. Figure 1b shows dominant RF power absorption by a small amount of ^{3}He ions, down to concentrations $X[^3\text{He}] \approx 0.1$–0.2%. Plasma heating with the three-ion D–(^{3}He)–H scenario at higher $X[^3\text{He}] \approx 0.5$–1% is equally possible. We note that the recipe

for the plasma composition given by equation (2) is valid for fast magnetosonic waves, excited at the low magnetic field side and propagating towards regions with increasing B, as in most of present-day fusion machines.

Efficient plasma heating with three-ion ICRH scenarios

A series of dedicated experiments were performed on the Alcator C-Mod tokamak[12] (MIT, Cambridge, USA; major radius $R_0 \approx 0.67$ m, minor radius $a_{pl} \approx 0.23$ m) and on the world-largest magnetic fusion device JET (Joint European Torus, Culham, UK; $R_0 \approx 3$ m, $a_{pl} \approx 1$ m). The goal of these studies was to demonstrate that indeed a small amount of ^{3}He ions can efficiently absorb RF power in H–D mixtures. The Alcator C-Mod experiments were run at high central electron densities $n_{e0} \approx (2$–$3) \times 10^{20}$ m^{-3} and very high toroidal magnetic field $B_0 = 7.8$ T at a plasma current $I_p = 1.2$ MA. In the JET experiments, $n_{e0} \approx 4 \times 10^{19}$ m^{-3} and $B_0 = 3.2$ T, $I_p = 2.0$ MA were used. Accordingly, ICRH frequencies $f = \omega/2\pi = 78.0$–80.0 MHz (Alcator C-Mod) and $f = 32.2$–33.0 MHz (JET) were chosen to locate the ^{3}He cyclotron resonance in the plasma centre in both devices. The Alcator C-Mod plasmas were heated with 4–5 MW of ICRH power only. In JET plasmas, 3.2 MW of neutral beam injection (NBI) was added prior to applying $\sim$4 MW of ICRH.

Figure 2 shows the time evolution of the central electron temperature T_{e0} and plasma stored energy W_p in response to the applied ICRH on Alcator C-Mod and on JET. These results confirm our earlier predictions (Fig. 1b) for the efficiency of ^{3}He absorption at concentrations of a few per mille (‰) in H–D plasmas. The optimal ^{3}He concentration for this scenario in C-Mod plasmas was approximately $X[^3\text{He}] \approx 0.5$%. In JET, even lower ^{3}He concentrations $\sim$0.2% were successfully applied.

In JET experiments, the edge isotopic ratio H/(H + D) was varied between 0.73 and 0.92 and the ^{3}He concentration between 0.1% and 1.5% to assess the sensitivity of ICRH on the detailed plasma composition. The core hydrogen concentration was estimated from the measured edge H/(H + D) ratio as $X[\text{H}] \approx 0.9 \times \text{H}/(\text{H} + \text{D})$, accounting for the presence of impurities in the plasma and additional D core fuelling from the D-NBI system. We find efficient
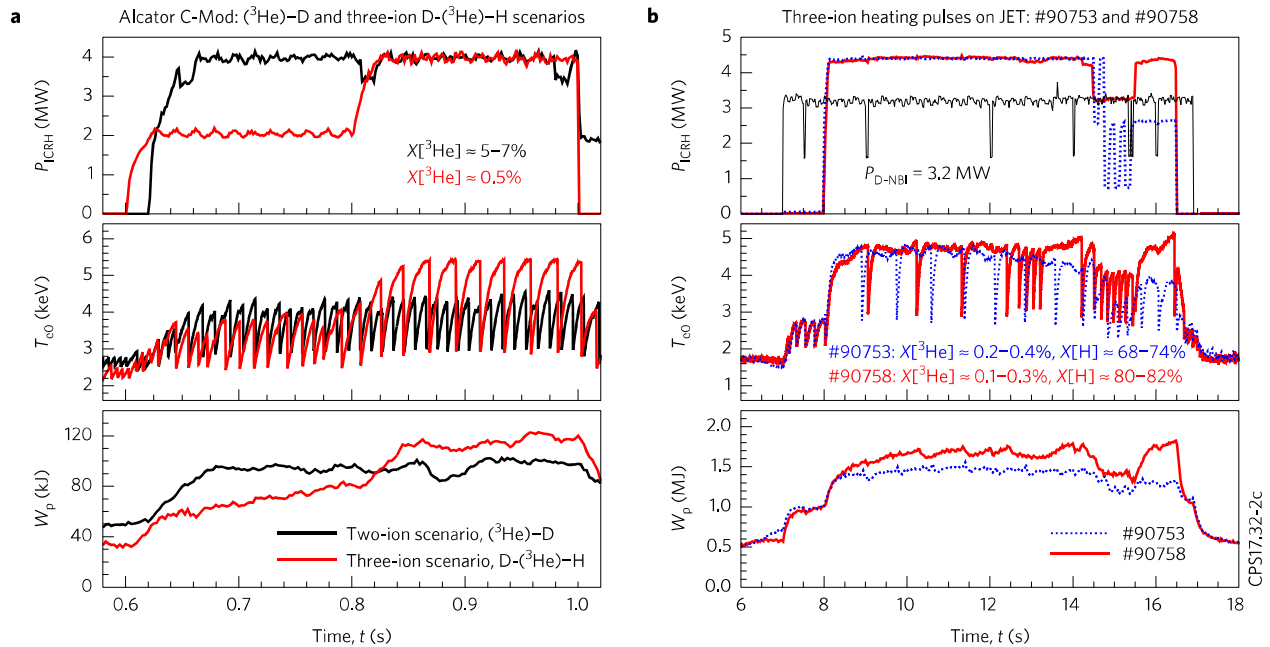
Figure 2 | Illustration of the performance of the D-(^{3}He)-H three-ion ICRH scenario on Alcator C-Mod and JET tokamaks. a, Alcator C-Mod three-ion heating pulse (#1160901009, $X[^3He] \approx 0.5\%$, red) and (^{3}He)-D pulse (#1160823003, $X[^3He] \approx 5$-7%, black). **b**, JET three-ion heating pulses #90753 ($X[H] \approx 68$-74%, $X[^3He] \approx 0.2$-0.4%, blue) and #90758 ($X[H] \approx 80$-82%, $X[^3He] \approx 0.1$-0.3%, red). Whereas a few % of ^{3}He is needed for minority heating in H or D majority plasmas, strong wave absorption in H-D plasmas is achieved with about ten times less ^{3}He.

plasma heating for a fairly broad range of the isotopic ratio (see also Supplementary Figs 5 and 6). In particular, central plasma heating with $\Delta T_{e0}/\Delta P_{ICRH} > 0.5$ keV MW^{-1} was observed for H/(H + D) $\approx$ 0.78-0.91 mixtures at ^{3}He concentrations below 0.5%.

Figure 2a also includes the evolution of T_{e0} and W_p for ^{3}He minority heating in the Alcator C-Mod D plasma with $X[^3He] \approx 5$-7% (pulse 1160823003). Compared to this (^{3}He)-D scenario, the three-ion heating scenario in C-Mod showed a larger increase in the plasma stored energy ($\Delta W_p/\Delta P_{ICRH} = 22$ kJ MW^{-1} versus 14 kJ MW^{-1}).

A direct comparison of the heating performance of the three-ion discharges was not possible for the JET discharges discussed here. However, it can be assessed comparing the measured thermal plasma energy to that derived from a so-called scaling law. These scaling laws predict the energy confinement value for a given plasma experiment as a function of specific engineering parameters (I_p, B_0, n_e, ...; ref. 13) and result from a statistical analysis of data collected from multiple tokamaks worldwide. Here, we use the well-established ITERL96-P and IPB98(y,2) scalings for the energy confinement time τ_E (equations (24) and (20) in ref. 13) for L-mode and H-mode tokamak plasmas. τ_E is the characteristic time during which the plasma maintains its energy if the heating power is suddenly switched off[1]. Under stationary conditions it is given by the ratio of the stored plasma energy divided by the total heating power. Supplementary Figs 1-4 show the results obtained for L-mode JET discharges heated with different ICRH minority scenarios, including the ratios $\tau_E/\tau_{E,scaling}$. From the definition of τ_E given above, it follows immediately that $\tau_E/\tau_{E,scaling}$ is equal to the ratio of the corresponding stored energies. For the three-ion heating pulse #90758 (Fig. 2b), we obtain $\tau_E/\tau_{IPB98(y,2)} \approx 0.85$-0.88 and $\tau_E/\tau_{ITERL96-P} \approx 1.43$-1.48. This compares very well to $\tau_E/\tau_{E,scaling}$ values for the excellent (H)-D minority heating scenario in JET plasmas (Supplementary Fig. 1).

Efficient generation of high-energy ions

Energetic ions play a crucial role in fusion plasmas[14]. Indeed, the success of magnetic fusion relies upon good confinement of fast alpha particles (^{4}He ions with birth energies 3.5 MeV). This is required to sustain high plasma temperatures and for economical operation of a fusion reactor[1]. However, these energetic ^{4}He ions can also trigger instabilities that degrade the plasma performance. To mimic the behaviour of fusion-born alphas, but without actually using D-T plasmas, ICRH has been extensively used in the past.

For fundamental ion cyclotron absorption the acquired ion energies scale with the absorbed RF power per particle[15]. Since three-ion scenarios allow minimizing the number of resonant particles down to ‰ levels, ions with rather high energies can be generated. For plasma densities and ICRH power levels available in the JET and C-Mod experiments, self-consistent power deposition computations with the codes AORSA[16], PION[17] and SCENIC[18] predicted acceleration of ^{3}He ions to energies of a few MeV.

Figure 2b shows fast repetitive drops in T_{e0} (so-called 'sawtooth' oscillations) with a period of $\sim$0.2 s during the NBI-only phase of JET pulses #90753 and #90758 ($t = 7$-8 s). Extended sawtooth periods up to $\sim$1.0 s are seen when ICRH is applied on top of NBI. Similarly, in the three-ion Alcator C-Mod discharge in Fig. 2a, the sawtooth period increases from $\sim$0.13 s during the 2 MW ICRH phase to $\sim$0.23 s during the 4 MW phase. The observation of long-period sawteeth is a first indication of the creation of energetic ions by ICRH, as the presence of fast ions in a plasma is well known to have a stabilizing effect on sawteeth[19,20].

An independent confirmation of accelerating ^{3}He ions to high energies is provided by gamma-ray emission spectroscopy on JET[21,22]. Figure 3a shows the gamma-ray spectrum for pulse #90753 during $t = 8$-14 s ($P_{ICRH} = 4.4$ MW), recorded with the LaBr$_3$ spectrometer[23]. The observed lines originate from ^{9}Be(^{3}He, $p\gamma$)^{11}B and ^{9}Be(^{3}He, $n\gamma$)^{11}C nuclear reactions between fast ^{3}He ions and beryllium (^{9}Be) impurities. These impurities are intrinsically present in JET plasmas with the ITER-like wall. The reported plasmas were contaminated with $\sim$0.5% ^{9}Be, as estimated by charge exchange measurements.

The observation of the $E_\gamma \approx 4.44$ MeV line implies immediately the presence of confined fast ^{3}He ions with energies >0.9 MeV (ref. 21). Alpha particles, born in concurrent ^{3}He-D fusion reactions, also contribute to the gamma-emission at this energy
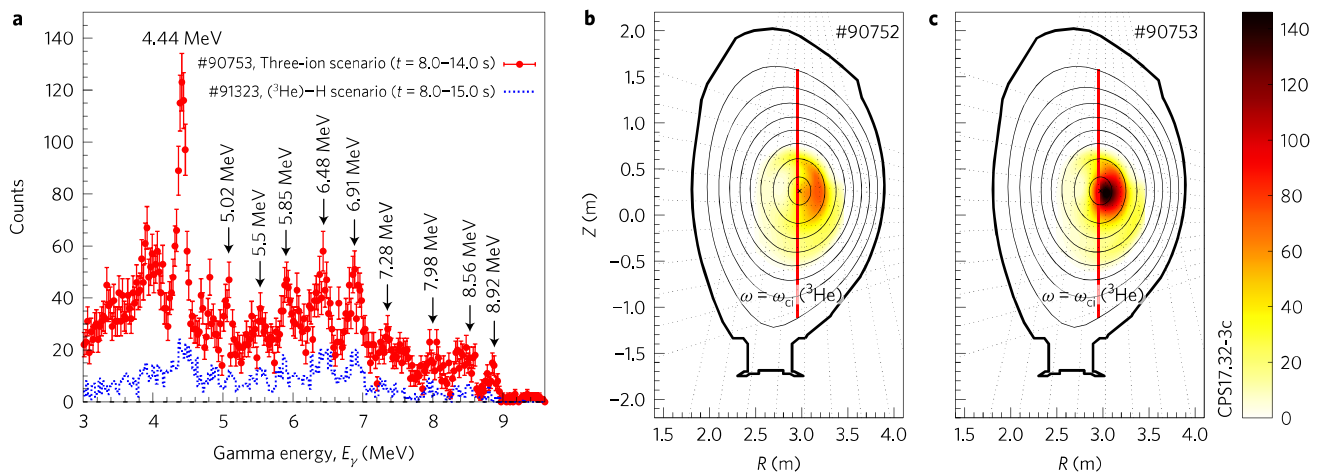
Figure 3 | Gamma-ray emission from ^{3}He + ^{9}Be nuclear reactions, proving the presence of energetic ICRH-accelerated ^{3}He ions. a, Gamma-ray spectra measured in JET pulse #90753 (three-ion scenario, $X[^3\text{He}] \approx 0.2$–$0.4\%$, red) and in pulse #91323 ((^{3}He)–H scenario, $X[^3\text{He}] \approx 1$–2%, blue). The error bars represent the square root of the number of counts in each channel of the spectrum and arise from the underlying Poisson statistics of the gamma-ray detection process. **b,c**, The JET plasma cross-section and 19 lines-of-sight of the neutron/gamma camera. The reconstructed high-energy gamma-ray emission ($E_\gamma = 4.5$–9.0 MeV) visualizes the population of the confined energetic ^{3}He ions ($E[^3\text{He}] > 1$–2 MeV). Pulses #90752 (**b**) and #90753 (**c**) had a nearly identical plasma composition ($X[\text{H}] \approx 70$–75%, $X[^3\text{He}] \approx 0.2$–$0.4\%$) and RF heating power ($P_{\text{ICRH}} = 4.3$–$4.4$ MW), except for the ICRH antenna phasing. A factor-of-two increase in the γ-ray emissivity was observed in pulse #90753, in which 2 MW of RF power was coupled to the plasma with $+\pi/2$ phasing (see text for more details).

through ^{4}He + ^{9}Be reactions. Figure 3a also shows a number of characteristic gamma lines at $E_\gamma > 4.44$ MeV, originating from transitions between higher excited states of ^{11}B and ^{11}C nuclei (products of ^{3}He + ^{9}Be reactions). The excitation efficiency for such high-energy levels increases by a factor of ten when the energy of the projectile ^{3}He ions increases from 1 MeV to 2 MeV (ref. 24). For comparison, we also display the γ-spectrum recorded in JET pulse #91323, in which ^{3}He ions (≈ 1–2%) were heated as a minority with up to 7.6 MW of ICRH in an almost pure H plasma (see Supplementary Fig. 3). Figure 3a clearly shows higher gamma-count rates for the three-ion pulse #90753 ($X[^3\text{He}] \approx 0.2$–$0.4\%$), although a factor of two less ICRH power was injected into the plasma.

In JET, we further enhanced the efficiency for fast-ion generation by changing the configuration of ICRH antennas from dipole to $+\pi/2$ phasing. The phasing defines the dominant $k_\parallel$ and the spectrum of emitted waves, where $k_\parallel$ is the wavenumber parallel to B. The $+\pi/2$ phasing launches waves predominantly in the direction of the plasma current with typical values $|k_\parallel^{(\text{ant})}| \approx 3.4\,\text{m}^{-1}$, which is two times smaller than for dipole phasing ($|k_\parallel^{(\text{ant})}| \approx 6.7\,\text{m}^{-1}$). Since the width of the absorption zone scales with $|k_\parallel|$, reducing it has the advantage of increasing the absorbed RF power per ion. Furthermore, the $+\pi/2$ phasing allows one to exploit the RF-induced pinch effect, beneficial to localize the energetic ions towards the plasma core[25].

The result is clearly visible in Fig. 3b,c, showing the two-dimensional tomographic reconstruction of the $E_\gamma = 4.5$–9.0 MeV gamma-ray emission[21] for two comparable three-ion heating pulses #90752 and #90753. Both had a similar edge H/(H + D) ratio, varying from ~0.84 at the beginning of the pulse to ~0.75 at the end ($X[\text{H}] \approx 68$–76%), and $X[^3\text{He}] \approx 0.2$–$0.4\%$. In pulse #90752 (Fig. 3b), all ICRH power was applied using dipole phasing, while in pulse #90753 (Fig. 3c) about half of the ICRH power (2.1 MW) was launched with $+\pi/2$ phasing. Energetic ^{3}He ions are more centrally localized and the number of gamma-ray counts increases by a factor of two in pulse #90753. The period of the sawtooth oscillations also increases from ~0.54 s to ~0.78 s.

We also observed excitation of Alfvén eigenmodes (AE) in JET plasmas with frequencies ≈ 320–340 kHz in pulses, where $P_{\text{ICRH}} \geq 2$ MW was delivered with $+\pi/2$ phasing. These instabilities

are excited if a sufficiently large number of energetic ions with velocities comparable to the Alfvén velocity is present in the plasma. Figure 4a shows the AE dynamics for JET pulse #90758 (previously shown in Fig. 2b), with a sequential excitation of modes with mode numbers from $n = 8$ to $n = 5$ during a long-period sawtooth. The MHD code MISHKA[26] yields eigenfrequencies $f_{\text{AE}}^{(0)} \approx 285$–$295$ kHz for $n = 5$–7 modes in the plasma frame. Even closer correspondence to the observations is obtained when plasma rotation due to NBI ($f_{\text{rot}} \approx 5$ kHz measured at $R \approx 3.25$ m) is taken into account ($f_{\text{AE}}^{(\text{lab})} = f_{\text{AE}}^{(0)} + n f_{\text{rot}} \approx 320$ kHz). Further analysis of the conditions for energetic ions to interact with the $n = 5$ AE mode yields ^{3}He ions with energies ≈ 1.5–2.5 MeV.

A similar AE activity was also detected in the Alcator C-Mod experiments during a sawtooth cycle with a period extended up to ~40 ms ($P_{\text{ICRH}} = 5$ MW). As shown in Fig. 4b, AEs at frequencies $f_{\text{AE}} \approx 1{,}270$–$1{,}300$ kHz ($n \approx 12$) were observed 30 ms after the sawteeth crash. Interestingly, the normalized frequency ratio $f_{\text{AE}}/f_{\text{A}}(0) \approx 0.56$–$0.61$ is similar for the AE modes observed on both devices. Here, $f_{\text{A}}(0) = v_{\text{A}}(0)/2\pi R_0$, with $v_{\text{A}}(0)$ the on-axis Alfvén velocity. This further highlights the similarity of the three-ion heating experiments on the two devices.

How many 'three-ion' scenarios exist?
These novel scenarios allow great flexibility in the choice of the three ion components. Table 1 summarizes the (Z/A) values for fusion-relevant ion species. The isotopes of hydrogen have $Z/A = 1$ (protons), $1/2$ (D ions) and $1/3$ (T ions). Fusion plasmas can also contain ^{4}He and light impurity species, released in plasma–wall interactions. In the core of high-temperature plasmas, those ions (^{4}He, ^{12}C, ^{16}O, and so on) are typically fully ionized with $Z/A = 1/2$, just as the D ions. We also note the isotope ^{3}He, which has a unique $Z/A = 2/3$. Other ion species such as ^{9}Be^{4+}, ^{7}Li^{3+}, ^{22}Ne^{10+}, and so on have a Z/A ratio in the range 0.43 and 0.45, and bring extra possibilities. Among these, beryllium is of particular importance. Plasmas in JET and the future tokamak ITER naturally contain a small amount of ^{9}Be impurities. Since $(Z/A)_{\text{T}} < (Z/A)_{9\text{Be}} < (Z/A)_{\text{D}}$, ^{9}Be ions can efficiently absorb RF power and transfer most of their energy to D and T ions during their collisional slowing-down, a feature particularly attractive for
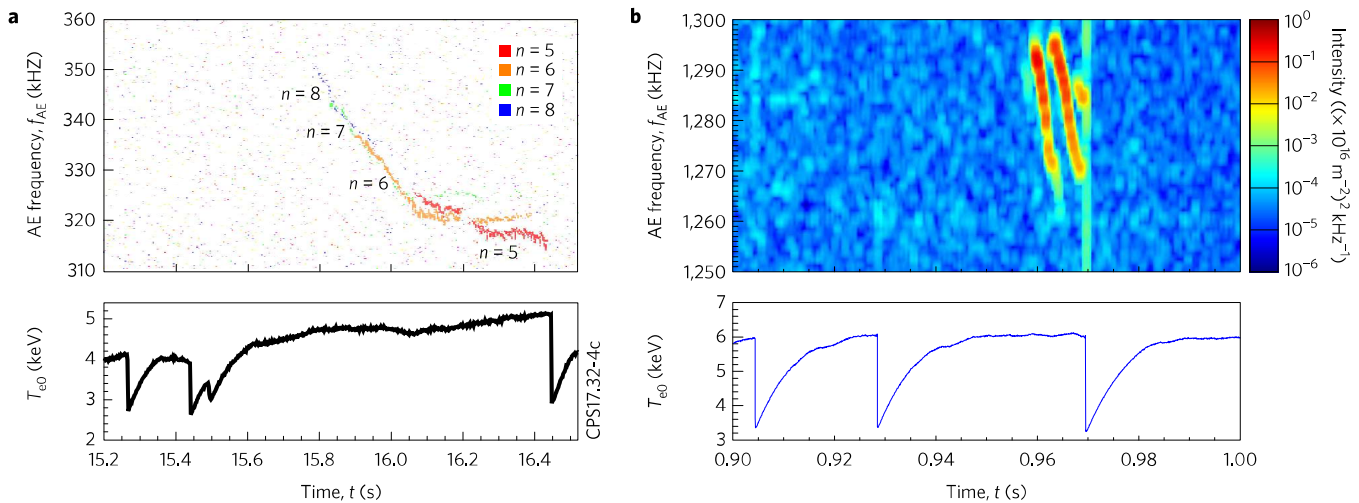
Figure 4 | Excitation of Alfvénic eigenmodes in magnetic fluctuation spectrograms, another proof of the presence of ICRH-accelerated fast ions.
a, JET pulse #90758. **b**, Alcator C-Mod pulse #1160901023. The evolution of the central electron temperature T_{e0} is also plotted in the bottom part of the figures.
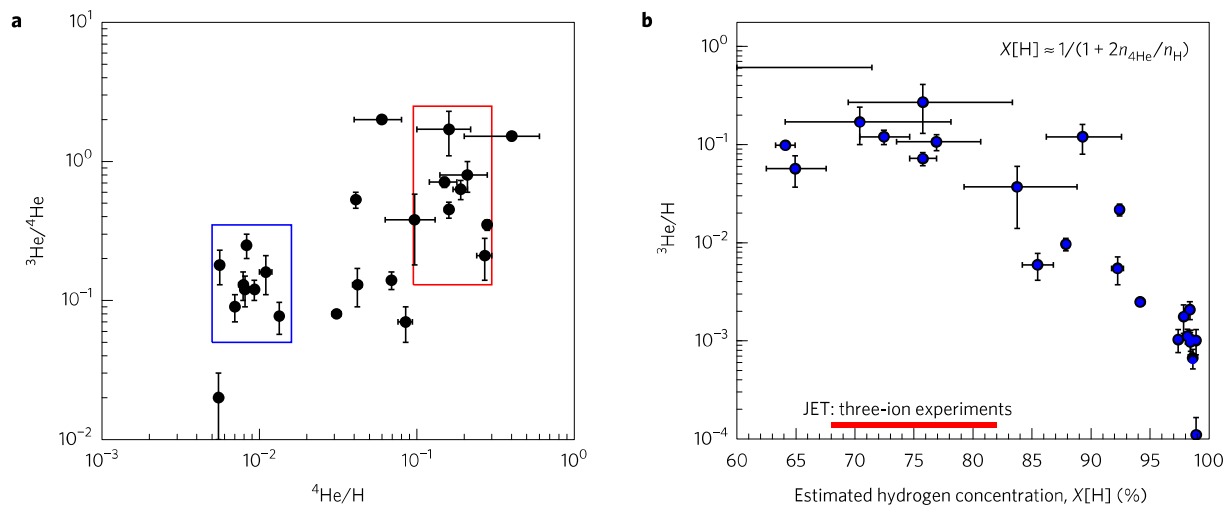

Figure 5 | Three-ion ICRH scenarios also explain some of the observations of energetic ions in space environments, in particular, ^{3}He-rich solar flares.
a, ^{4}He/H and ^{3}He/^{4}He ratios for ^{3}He-rich solar flares. Data taken from Table 1 and Fig. 2 of ref. 32, including the original error bars. The data cloud within the red line corresponds to a $n_{^4He}/n_H$ ratio very similar to our theoretical predictions for a hypothetical three-ion ^{4}He–(^{3}He)–H scenario at work in space plasmas (see text for more details). **b**, The ratio $n_{^3He}/n_H = (n_{^3He}/n_{^4He}) \times (n_{^4He}/n_H)$, measured in the MeV-energy range, versus H concentration estimated from $X[H] \approx 1/(1 + 2n_{^4He}/n_H)$ for the same dataset (ref. 32). A large ^{3}He enhancement for the events at $X[H] \approx 70$–75% is seen. The error bars for $n_{^3He}/n_H$ are directly taken from Table 1 of ref. 32. The error bars for the estimated H concentration are computed using the relation between $X[H]$ and $n_{^4He}/n_H$, and taking the maximum and minimum values of $n_{^4He}/n_H$ for a particular ^{3}He-rich event.

Table 1 | (Z/A) ratio for different ion species in fusion plasmas.

Ion species	T	^{9}Be, ^{7}Li, ^{22}Ne	D, ^{4}He, ^{12}C, . . .	^{3}He	H
$(Z/A)_i$	1/3	$\approx$0.43–0.45	1/2	2/3	1

a fusion reactor[10]. As another example of the three-ion technique, we mention the observed parasitic off-axis absorption of ICRH power by ^{7}Li impurities in D–T plasmas of the Tokamak Fusion Test Reactor[27]. Low-temperature plasmas offer an even larger variety of scenarios since light ion species are not necessarily fully ionized.

Relevance for space plasmas

As discussed above, ion species with $Z/A = 1/2$ are nearly identical to D ions from the wave propagation point of view. Therefore,

helium ions ($Z = 2$, $A = 4$) can replace D. According to equation (2) and Fig. 2b, hydrogen plasmas additionally including 10–17% of ^{4}He ions are optimal for effective RF power absorption by a small amount of ^{3}He ions.

The presented experimental results provide also an additional insight into the understanding of the ^{3}He-rich solar flares[28–30], known for the past four decades. These events are characterized by an anomalously large abundance ratio ^{3}He/^{4}He $\sim$ 1 in the energy range $\sim$1 MeV/nucleon, compared with a typical value of ^{3}He/^{4}He $\sim 5 \times 10^{-4}$ in the solar corona. The proposed theoretical models to explain anomalous ^{3}He-enrichment generally rely on selective energy absorption by these ions via wave interaction mechanisms making use of the unique charge-to-mass ratio of ^{3}He.

Fisk suggested pre-heating of ^{3}He ions via electrostatic ion cyclotron waves in H–^{4}He plasmas, followed by a second-stage acceleration process[28]. Crucial in his model for the wave absorption

by ^{3}He ions is also having a plasma mixture, consisting of H and ^{4}He ions. On the other hand, Reames highlights in his review (ref. 30) that the ^{3}He-rich events are associated with streaming 10–100 keV electrons. He suggests that such electron beams might be a source for electromagnetic ion cyclotron waves. The advantage of this explanation is that electromagnetic waves can directly accelerate ions to MeV energies, without the need of a secondary process, which is a serious simplification compared to the theory by Fisk. Roth and Temerin developed a single-stage model for the resonant acceleration of ^{3}He ions to high energies, utilizing electromagnetic ion cyclotron waves in H plasmas[31]. Their study resembles closely the (^{3}He)–H minority heating in tokamaks. Figure 3a, showing the γ-ray spectrum for JET pulse #91323, confirms generation of MeV-range ^{3}He ions with this scenario in a fusion hydrogen plasma.

Figure 3a also illustrates that a significantly larger number of high-energy ^{3}He ions was generated using the D–(^{3}He)–H three-ion scenario under similar conditions. Thus, we hypothesize that resonant absorption of electromagnetic waves by a small amount of ^{3}He ions in H–^{4}He plasmas (that is, effectively the three-ion ^{4}He–(^{3}He)–H scenario) can be another effective mechanism for ^{3}He acceleration in space plasmas. This proposal then combines in one scenario the advantages of the theories of Fisk and Temerin–Roth. We recall that in JET experiments efficient RF power absorption by ^{3}He ions was observed in H–D plasmas with $X[\text{H}] \approx 68\%$–82% (see Fig. 2b and Supplementary Figs 5 and 6). Equivalent H–^{4}He mixtures with the same H concentrations should have a $n_{^4\text{He}}/n_\text{H}$ ratio in the range between 0.11 and 0.24.

Figure 5a summarizes the ^{4}He/H and ^{3}He/^{4}He ratios for a number of observed ^{3}He-rich solar flares, taken from Table 1 and Fig. 2 of ref. 32. Remarkably, our estimates are consistent with the data points at $n_{^4\text{He}}/n_\text{H} \approx 0.1$–0.3. This becomes even clearer if the same dataset is plotted as a function of the estimated hydrogen concentration $X[\text{H}] \approx 1/(1 + 2n_{^4\text{He}}/n_\text{H})$ and using the measured number of energetic ^{3}He ions normalized to the number of protons, $n_{^3\text{He}}/n_\text{H}$, as an indicator for the efficiency of ^{3}He acceleration. Figure 5b shows a large ^{3}He enhancement for events with $X[\text{H}] \approx 70$–75%, thus providing additional support for our hypothesis.

Data availability. The data that support the plots within this paper and other findings of this study are available from the corresponding author upon reasonable request.

References

1. Ongena, J. et al. Magnetic-confinement fusion. *Nat. Phys.* **12**, 398–410 (2016).
2. Adam, J. Review of tokamak plasma heating by wave damping in the ion cyclotron range of frequency. *Plasma Phys. Control. Fusion* **29**, 443–472 (1987).
3. Porkolab, M. et al. Recent progress in ICRF physics. *Plasma Phys. Control. Fusion* **40**, A35–A52 (1998).
4. Noterdaeme, J.-M. et al. Physics studies with the additional heating systems in JET. *Fusion Sci. Tech.* **53**, 1103–1151 (2008).
5. Lerche, E. et al. Optimization of ICRH for core impurity control in JET-ILW. *Nucl. Fusion* **56**, 036022 (2016).
6. Van Eester, D. et al. JET (^{3}He)–D scenarios relying on RF heating: survey of selected recent experiments. *Plasma Phys. Control. Fusion* **51**, 044007 (2009).
7. Mantsinen, M. J. et al. Localized bulk electron heating with ICRF mode conversion in the JET tokamak. *Nucl. Fusion* **44**, 33–46 (2004).
8. Kazakov, Ye. O. et al. On resonant ICRF absorption in three-ion component plasmas: a new promising tool for fast ion generation. *Nucl. Fusion* **55**, 032001 (2015).
9. Kazakov, Ye. O. et al. Fast ion generation and bulk plasma heating with three-ion ICRF scenarios. *AIP Conf. Proc.* **1689**, 030008 (2015).
10. Kazakov, Ye. O. et al. A new ion cyclotron range of frequency scenario for bulk ion heating in deuterium–tritium plasmas: How to utilize intrinsic impurities in our favour. *Phys. Plasmas* **22**, 082511 (2015).
11. Van Eester, D. & Koch, R. A variational principle for studying fast-wave mode conversion. *Plasma Phys. Control. Fusion* **40**, 1949–1975 (1998).
12. Marmar, E. S. et al. Alcator C-Mod: research in support of ITER and steps beyond. *Nucl. Fusion* **55**, 104020 (2015).
13. ITER Physics Expert Groups on Confinement and Transport et al., Chapter 2: Plasma confinement and transport. *Nucl. Fusion* **39**, 2175–2249 (1999).
14. Breizman, B. N. & Sharapov, S. E. Major minority: energetic particles in fusion plasmas. *Plasma Phys. Control. Fusion* **53**, 054001 (2011).
15. Stix, T. H. Fast-wave heating of a two-component plasma. *Nucl. Fusion* **15**, 737–754 (1975).
16. Jaeger, E. F. et al. Advances in full-wave modeling of radio frequency heated, multidimensional plasmas. *Phys. Plasmas* **9**, 1873–1881 (2002).
17. Eriksson, L.-G. et al. ICRF heating of JET plasmas with the third harmonic deuterium resonance. *Nucl. Fusion* **38**, 265–278 (1998).
18. Jucker, M. Integrated modeling for ion cyclotron resonant heating in toroidal systems. *Comput. Phys. Commun.* **182**, 912–925 (2011).
19. Porcelli, F. et al. Model for the sawtooth period and amplitude. *Plasma Phys. Control. Fusion* **38**, 2163–2186 (1996).
20. Graves, J. P. et al. Control of magnetohydrodynamic stability by phase space engineering of energetic ions in tokamak plasmas. *Nat. Commun.* **3**, 624 (2012).
21. Kiptily, V. G. et al. Gamma ray diagnostics of high temperature magnetically confined fusion plasmas. *Plasma Phys. Control. Fusion* **48**, R59–R82 (2006).
22. Tardocchi, M. et al. Diagnosis of physical parameters of fast particles in high power fusion plasmas with high resolution neutron and gamma-ray spectroscopy. *Plasma Phys. Control. Fusion* **55**, 074014 (2013).
23. Nocente, M. et al. High resolution gamma ray spectroscopy at MHz counting rates with LaBr$_3$ scintillators for fusion plasma applications. *IEEE Trans. Nucl. Sci.* **60**, 1408–1415 (2013).
24. Coker, W. R. et al. An investigation of the ^{9}Be(^{3}He, p)^{11}B reaction at low energies. *Nucl. Phys. A* **91**, 97–111 (1967).
25. Mantsinen, M. J. et al. Controlling the profile of ion-cyclotron-resonant ions in JET with the wave-induced pinch effect. *Phys. Rev. Lett.* **89**, 115004 (2002).
26. Mikhailovskii, A. B. et al. Optimization of computational MHD normal-mode analysis in tokamaks. *Plasma Phys. Rep.* **23**, 844–857 (1997).
27. Wilson, J. R. et al. Ion cyclotron range of frequencies heating and flow generation in deuterium–tritium plasmas. *Phys. Plasmas* **5**, 1721–1726 (1998).
28. Fisk, L. A. ^{3}He-rich flares: a possible explanation. *Astrophys. J.* **224**, 1048–1055 (1978).
29. Kocharov, L. G. & Kocharov, G. E. ^{3}He-rich solar flares. *Space Sci. Rev.* **38**, 89–141 (1984).
30. Reames, D. V. Particle acceleration at the sun and in the heliosphere. *Space Sci. Rev.* **90**, 413–491 (1999).
31. Roth, I. & Temerin, M. Enrichment of ^{3}He and heavy ions in impulsive solar flares. *Astrophys. J.* **477**, 940–957 (1997).
32. Ramadurai, S. et al. ^{3}He-rich solar flares. *Pramana – J. Phys.* **23**, 305–311 (1984).
33. Litaudon, X. et al. Overview of the JET results in support to ITER. *Nucl. Fusion* (in the press).

Author contributions

All authors have contributed to the publication, being variously involved in the design of the experiments, in running the diagnostics, acquiring data and finally analysing the processed data.

Alcator C-Mod Team

E. S. Marmar[1], S. G. Baek[1], H. Barnard[1], P. Bonoli[1], D. Brunner[1], J. Candy[2], J. Canik[3], R. M. Churchill[4], I. Cziegler[5], G. Dekow[1], L. Delgado-Aparicio[4], A. Diallo[4], E. Edlund[4], P. Ennever[1], I. Faust[1], C. Fiore[1], Chi Gao[1], T. Golfinopoulos[1], M. Greenwald[1], Z. S. Hartwig[1], C. Holland[5], A. E. Hubbard[1], J. W. Hughes[1], I. H. Hutchinson[1], J. Irby[1], B. LaBombard[1], Yijun Lin[1], B. Lipschultz[6], A. Loarte[7], R. Mumgaard[1], R. R. Parker[1], M. Porkolab[1], M. L. Reinke[6], J. E. Rice[1], S. Scott[4], S. Shiraiwa[1], P. Snyder[2], B. Sorbom[1], D. Terry[1], J. L. Terry[1], C. Theiler[8], R. Vieira[1], J. R. Walk[1], G. M. Wallace[1], A. White[1], D. Whyte[1], S. M. Wolfe[1], G. M. Wright[1], J. Wright[1], S. J. Wukitch[1] and P. Xu[1]

---

[1]Plasma Science and Fusion Center, Massachusetts Institute of Technology, Cambridge, Massachusetts, USA. [2]General Atomics, San Diego, California, USA. [3]Oak Ridge National Laboratory, Oak Ridge, Tennessee, USA. [4]Princeton Plasma Physics Laboratory, Princeton, New Jersey, USA. [5]Center for Energy Research, University of California San Diego, San Diego, California, USA. [6]Department of Physics, University of York, York, USA. [7]Plasma Operations Directorate, ITER Organization, St. Paul lez Durance, France. [8]TCV Tokamak Physics, Centre de Recherches en Physique des Plasmas, Lausanne, Switzerland.

JET Contributors

S. Abduallev[39], M. Abhangi[46], P. Abreu[53], M. Afzal[7], K. M. Aggarwal[29], T. Ahlgren[101], J. H. Ahn[8], L. Aho-Mantila[112], N. Aiba[69], M. Airila[112], R. Albanese[105], V. Aldred[7], D. Alegre[93], E. Alessi[45], P. Aleynikov[55], A. Alfier[12], A. Alkseev[72], M. Allinson[7], B. Alper[7], E. Alves[53], G. Ambrosino[105], R. Ambrosino[106], L. Amicucci[90], V. Amosov[88], E. Andersson Sundén[22], M. Angelone[90], M. Anghel[85], C. Angioni[62], L. Appel[7], C. Appelbee[7], P. Arena[30], M. Ariola[106], H. Arnichand[8], S. Arshad[41], A. Ash[7], N. Ashikawa[68], V. Aslanyan[64], O. Asunta[1], F. Auriemma[12], Y. Austin[7], L. Avotina[103], M. D. Axton[7], C. Ayres[7], M. Bacharis[24], A. Baciero[57], D. Baião[53], S. Bailey[7], A. Baker[7], I. Balboa[7], M. Balden[62], N. Balshaw[7], R. Bament[7], J. W. Banks[7], Y. F. Baranov[7], M. A. Barnard[7], D. Barnes[7], M. Barnes[27], R. Barnsley[55], A. Baron Wiechec[7], L. Barrera Orte[34], M. Baruzzo[12], V. Basiuk[8], M. Bassan[55], R. Bastow[7], A. Batista[53], P. Batistoni[90], R. Baughan[7], B. Bauvir[55], L. Baylor[73], B. Bazylev[56], J. Beal[110], P. S. Beaumont[7], M. Beckers[39], B. Beckett[7], A. Becoulet[8], N. Bekris[35], M. Beldishevski[7], K. Bell[7], F. Belli[90], M. Bellinger[7], É. Belonohy[62], N. Ben Ayed[7], N. A. Benterman[7], H. Bergsåker[42], J. Bernardo[53], M. Bernert[62], M. Berry[7], L. Bertalot[55], C. Besliu[7], M. Beurskens[63], B. Bieg[61], J. Bielecki[47], T. Biewer[73], M. Bigi[12], P. Bílková[50], F. Binda[22], A. Bisoffi[31], J. P. S. Bizarro[53], C. Björkas[101], J. Blackburn[7], K. Blackman[7], T. R. Blackman[7], P. Blanchard[33], P. Blatchford[7], V. Bobkov[62], A. Boboc[7], G. Bodnár[113], O. Bogar[18], I. Bolshakova[60], T. Bolzonella[12], N. Bonanomi[97], F. Bonelli[56], J. Boom[62], J. Booth[7], D. Borba[35,53], D. Borodin[39], I. Borodkina[39], A. Botrugno[90], C. Bottereau[8], P. Boulting[7], C. Bourdelle[8], M. Bowden[7], C. Bower[7], C. Bowman[110], T. Boyce[7], C. Boyd[7], H. J. Boyer[7], J. M. A. Bradshaw[7], V. Braic[87], R. Bravanec[40], B. Breizman[107], S. Bremond[8], P. D. Brennan[7], S. Breton[8], A. Brett[7], S. Brezinsek[39], M. D. J. Bright[7], M. Brix[7], W. Broeckx[78], M. Brombin[12], A. Brosławski[65], D. P. D. Brown[7], M. Brown[7], E. Bruno[55], J. Bucalossi[8], J. Buch[46], J. Buchanan[7], M. A. Buckley[7], R. Budny[76], H. Bufferand[8], M. Bulman[7], N. Bulmer[7], P. Bunting[7], P. Buratti[90], A. Burckhart[62], A. Buscarino[30], A. Busse[7], N. K. Butler[7], I. Bykov[42], J. Byrne[7], P. Cahyna[50], G. Calabrò[90], I. Calvo[57], Y. Camenen[4], P. Camp[7], D. C. Campling[7], J. Cane[7], B. Cannas[17], A. J. Capel[7], P. J. Card[7], A. Cardinali[90], P. Carman[7], M. Carr[7], D. Carralero[62], L. Carraro[12], B. B. Carvalho[53], I. Carvalho[53], P. Carvalho[53], F. J. Casson[7], C. Castaldo[90], N. Catarino[53], J. Caumont[7], F. Causa[90], R. Cavazzana[12], K. Cave-Ayland[7], M. Cavinato[12], M. Cecconello[22], S. Ceccuzzi[90], E. Cecil[76], A. Cenedese[12], R. Cesario[90], C. D. Challis[7], M. Chandler[7], D. Chandra[46], C. S. Chang[76], A. Chankin[62], I. T. Chapman[7], S. C. Chapman[28], M. Chernyshova[49], G. Chitarin[12], G. Ciraolo[8], D. Ciric[7], J. Citrin[38], F. Clairet[8], E. Clark[7], M. Clark[7], R. Clarkson[7], D. Clatworthy[7], C. Clements[7], M. Cleverly[7], J. P. Coad[7], P. A. Coates[7], A. Cobalt[7], V. Coccorese[105], V. Cocilovo[90], S. Coda[33], R. Coelho[53], J. W. Coenen[39], I. Coffey[29], L. Colas[8], S. Collins[7], D. Conka[103], S. Conroy[22], N. Conway[7], D. Coombs[7], D. Cooper[7], S. R. Cooper[7], C. Corradino[30], Y. Corre[8], G. Corrigan[7], S. Cortes[53], D. Coster[62], A. S. Couchman[7], M. P. Cox[7], T. Craciunescu[86], S. Cramp[7], R. Craven[7], F. Crisanti[90], G. Croci[97], D. Croft[7], K. Crombé[15], R. Crowe[7], N. Cruz[53], G. Cseh[113], A. Cufar[81], A. Cullen[7], M. Curuia[85], A. Czarnecka[49], H. Dabirikhah[7], P. Dalgliesh[7], S. Dalley[7], J. Dankowski[47], D. Darrow[76], O. Davies[7], W. Davis[55,76], C. Day[56], I. E. Day[7], M. De Bock[55], A. de Castro[57], E. de la Cal[57], E. de la Luna[57], G. De Masi[12], J. L. de Pablos[57], G. De Temmerman[55], G. De Tommasi[105], P. de Vries[55], K. Deakin[7], J. Deane[7], F. Degli Agostini[12], R. Dejarnac[50], E. Delabie[73], N. den Harder[38], R. O. Dendy[7], J. Denis[8], P. Denner[39], S. Devaux[62,104], P. Devynck[8], F. Di Maio[55], A. Di Siena[62], C. Di Troia[90], P. Dinca[86], R. D'Inca[62], B. Ding[51], T. Dittmar[39], H. Doerk[62], R. P. Doerner[9], T. Donné[34], S. E. Dorling[7], S. Dormido-Canto[93], S. Doswon[7], D. Douai[8], P. T. Doyle[7], A. Drenik[62,81], P. Drewelow[63], P. Drews[39], Ph. Duckworth[55], R. Dumont[8], P. Dumortier[58], D. Dunai[113], M. Dunne[62], I. Ďuran[50], F. Durodié[58], P. Dutta[46], B. P. Duval[33], R. Dux[62], K. Dylst[78], N. Dzysiuk[22], P. V. Edappala[46], J. Edmond[7], A. M. Edwards[7], J. Edwards[7], Th. Eich[62], A. Ekedahl[8], R. El-Jorf[7], C. G. Elsmore[7], M. Enachescu[84], G. Ericsson[22], F. Eriksson[16], J. Eriksson[22], L. G. Eriksson[36], B. Esposito[90], S. Esquembri[94], H. G. Esser[39], D. Esteve[8], B. Evans[7], G. E. Evans[7], G. Evison[7], G. D. Ewart[7], D. Fagan[7], M. Faitsch[62], D. Falie[86], A. Fanni[17], A. Fasoli[33], J. M. Faustin[33], N. Fawlk[7], L. Fazendeiro[53], N. Fedorczak[8], R. C. Felton[7], K. Fenton[7], A. Fernades[53], H. Fernandes[53], J. Ferreira[53], J. A. Fessey[7], O. Février[8], O. Ficker[50], A. Field[7], S. Fietz[62], A. Figueiredo[53], J. Figueiredo[53,35], A. Fil[8], P. Finburg[7], M. Firdaouss[8], U. Fischer[56], L. Fittill[7], M. Fitzgerald[7], D. Flammini[90], J. Flanagan[7], C. Fleming[7], K. Flinders[7], N. Fonnesu[90], J. M. Fontdecaba[57], A. Formisano[79], L. Forsythe[7], L. Fortuna[30], E. Fortuna-Zalesna[19], M. Fortune[7], S. Foster[7], T. Franke[34],

T. Franklin[7], M. Frasca[30], L. Frassinetti[42], M. Freisinger[39], R. Fresa[98], D. Frigione[90], V. Fuchs[50], D. Fuller[35], S. Futatani[6], J. Fyvie[7], K. Gál[34,62], D. Galassi[2], K. Gałązka[49], J. Galdon-Quiroga[92], J. Gallagher[7], D. Gallart[6], R. Galvão[10], X. Gao[51], Y. Gao[39], J. Garcia[8], A. Garcia-Carrasco[42], M. García-Muñoz[92], J.-L. Gardarein[3], L. Garzotti[7], P. Gaudio[95], E. Gauthier[8], D. F. Gear[7], S. J. Gee[7], B. Geiger[62], M. Gelfusa[95], S. Gerasimov[7], G. Gervasini[45], M. Gethins[7], Z. Ghani[7], M. Ghate[46], M. Gherendi[86], J. C. Giacalone[8], L. Giacomelli[45], C. S. Gibson[7], T. Giegerich[56], C. Gil[8], L. Gil[53], S. Gilligan[7], D. Gin[54], E. Giovannozzi[90], J. B. Girardo[8], C. Giroud[7], G. Giruzzi[8], S. Glöggler[62], J. Godwin[7], J. Goff[7], P. Gohil[43], V. Goloborod'ko[102], R. Gomes[53], B. Gonçalves[53], M. Goniche[8], M. Goodliffe[7], A. Goodyear[7], G. Gorini[97], M. Gosk[65], R. Goulding[76], A. Goussarov[78], R. Gowland[7], B. Graham[7], M. E. Graham[7], J. P. Graves[33], N. Grazier[7], P. Grazier[7], N. R. Green[7], H. Greuner[62], B. Grierson[76], F. S. Griph[7], C. Grisolia[8], D. Grist[7], M. Groth[1], R. Grove[73], C. N. Grundy[7], J. Grzonka[19], D. Guard[7], C. Guérard[34], C. Guillemaut[8,53], R. Guirlet[8], C. Gurl[7], H. H. Utoh[69], L. J. Hackett[7], S. Hacquin[8,35], A. Hagar[7], R. Hager[76], A. Hakola[112], M. Halitovs[103], S. J. Hall[7], S.P. Hallworth Cook[7], C. Hamlyn-Harris[7], K. Hammond[7], C. Harrington[7], J. Harrison[7], D. Harting[7], F. Hasenbeck[39], Y. Hatano[108], D. R. Hatch[107], T. D. V. Haupt[7], J. Hawes[7], N. C. Hawkes[7], J. Hawkins[7], P. Hawkins[7], P. W. Haydon[7], N. Hayter[7], S. Hazel[7], P. J. L. Heesterman[7], K. Heinola[101], C. Hellesen[22], T. Hellsten[42], W. Helou[8], O. N. Hemming[7], T. C. Hender[7], M. Henderson[55], S. S. Henderson[21], R. Henriques[53], D. Hepple[7], G. Hermon[7], P. Hertout[8], C. Hidalgo[57], E. G. Highcock[27], M. Hill[7], J. Hillairet[8], J. Hillesheim[7], D. Hillis[73], K. Hizanidis[70], A. Hjalmarsson[22], J. Hobirk[62], E. Hodille[8], C. H. A. Hogben[7], G. M. D. Hogeweij[38], A. Hollingsworth[7], S. Hollis[7], D. A. Homfray[7], J. Horáček[50], G. Hornung[15], A. R. Horton[7], L. D. Horton[36], L. Horvath[110], S. P. Hotchin[7], M. R. Hough[7], P. J. Howarth[7], A. Hubbard[64], A. Huber[39], V. Huber[39], T. M. Huddleston[7], M. Hughes[7], G. T. A. Huijsmans[55], C. L. Hunter[7], P. Huynh[8], A. M. Hynes[7], D. Iglesias[7], N. Imazawa[69], F. Imbeaux[8], M. Imríšek[50], M. Incelli[109], P. Innocente[12], M. Irishkin[8], I. Ivanova-Stanik[49], S. Jachmich[58,35], A. S. Jacobsen[83], P. Jacquet[7], J. Jansons[103], A. Jardin[8], A. Järvinen[1], F. Jaulmes[38], S. Jednoróg[49], I. Jenkins[7], C. Jeong[20], I. Jepu[86], E. Joffrin[8], R. Johnson[7], T. Johnson[42], Jane Johnston[7], L. Joita[7], G. Jones[7], T. T. C. Jones[7], K. K. Hoshino[69], A. Kallenbach[62], K. Kamiya[69], J. Kaniewski[7], A. Kantor[7], A. Kappatou[62], J. Karhunen[1], D. Karkinsky[7], I. Karnowska[7], M. Kaufman[73], G. Kaveney[7], Y. Kazakov[58], V. Kazantzidis[70], D. L. Keeling[7], T. Keenan[7], J. Keep[7], M. Kempenaars[7], C. Kennedy[7], D. Kenny[7], J. Kent[7], O. N. Kent[7], E. Khilkevich[54], H. T. Kim[35], H. S. Kim[80], A. Kinch[7], C. king[7], D. King[7], R. F. King[7], D. J. Kinna[7], V. Kiptily[7], A. Kirk[7], K. Kirov[7], A. Kirschner[39], G. Kizane[103], C. Klepper[73], A. Klix[56], P. Knight[7], S. J. Knipe[7], S. Knott[96], T. Kobuchi[69], F. Köchl[111], G. Kocsis[113], I. Kodeli[81], L. Kogan[7], D. Kogut[8], S. Koivuranta[112], Y. Kominis[70], M. Köppen[39], B. Kos[81], T. Koskela[1], H. R. Koslowski[39], M. Koubiti[4], M. Kovari[7], E. Kowalska-Strzęciwilk[49], A. Krasilnikov[88], V. Krasilnikov[88], N. Krawczyk[49], M. Kresina[8], K. Krieger[62], A. Krivska[58], U. Kruezi[7], I. Książek[48], A. Kukushkin[72], A. Kundu[46], T. Kurki-Suonio[1], S. Kwak[20], R. Kwiatkowski[65], O. J. Kwon[13], L. Laguardia[45], A. Lahtinen[101], A. Laing[7], N. Lam[7], H. T. Lambertz[39], C. Lane[7], P. T. Lang[62], S. Lanthaler[33], J. Lapins[103], A. Lasa[101], J. R. Last[7], E. Łaszyńska[49], R. Lawless[7], A. Lawson[7], K. D. Lawson[7], A. Lazaros[70], E. Lazzaro[45], J. Leddy[110], S. Lee[66], X. Lefebvre[7], H. J. Leggate[32], J. Lehmann[7], M. Lehnen[55], D. Leichtle[41], P. Leichuer[7], F. Leipold[55,83], I. Lengar[81], M. Lennholm[36], E. Lerche[58], A. Lescinskis[103], S. Lesnoj[7], E. Letellier[7], M. Leyland[110], W. Leysen[78], L. Li[39], Y. Liang[39], J. Likonen[112], J. Linke[39], Ch. Linsmeier[39], B. Lipschultz[110], X. Litaudon[35], G. Liu[55], Y. Liu[51], V. P. Lo Schiavo[105], T. Loarer[8], A. Loarte[55], R. C. Lobel[7], B. Lomanowski[1], P. J. Lomas[7], J. Lönnroth[1,35], J. M. López[94], J. López-Razola[57], R. Lorenzini[12], U. Losada[57], J. J. Lovell[7], A. B. Loving[7], C. Lowry[36], T. Luce[43], R. M. A. Lucock[7], A. Lukin[74], C. Luna[5], M. Lungaroni[95], C. P. Lungu[86], M. Lungu[86], A. Lunniss[110], I. Lupelli[7], A. Lyssoivan[58], N. Macdonald[7], P. Macheta[7], K. Maczewa[7], B. Magesh[46], P. Maget[8], C. Maggi[7], H. Maier[62], J. Mailloux[7], T. Makkonen[1], R. Makwana[46], A. Malaquias[53], A. Malizia[95], P. Manas[4], A. Manning[7], M. E. Manso[53], P. Mantica[45], M. Mantsinen[6], A. Manzanares[91], Ph. Maquet[55], Y. Marandet[4], N. Marcenko[88], C. Marchetto[45], O. Marchuk[39], M. Marinelli[95], M. Marinucci[90], T. Marković[50], D. Marocco[90], L. Marot[26], C. A. Marren[7], R. Marshal[7], A. Martin[7], Y. Martin[33], A. Martín de Aguilera[57], F. J. Martínez[93], J. R. Martín-Solís[14], Y. Martynova[39], S. Maruyama[55], A. Masiello[12], M. Maslov[7], S. Matejcik[18], M. Mattei[79], G. F. Matthews[7], F. Maviglia[11], M. Mayer[62], M. L. Mayoral[34], T. May-Smith[7], D. Mazon[8], C. Mazzotta[90], R. McAdams[7], P. J. McCarthy[96], K. G. McClements[7], O. McCormack[12], P. A. McCullen[7], D. McDonald[34], S. McIntosh[7], R. McKean[7], J. McKehon[7], R. C. Meadows[7], A. Meakins[7], F. Medina[57], M. Medland[7], S. Medley[7], S. Meigh[7], A. G. Meigs[7], G. Meisl[62], S. Meitner[73], L. Meneses[53], S. Menmuir[7,42], K. Mergia[71], I. R. Merrigan[7], Ph. Mertens[39], S. Meshchaninov[88], A. Messiaen[58], H. Meyer[7], S. Mianowski[65], R. Michling[55], D. Middleton-Gear[7], J. Miettunen[1], F. Militello[7], E. Militello-Asp[7], G. Miloshevsky[77], F. Mink[62], S. Minucci[105], Y. Miyoshi[69], J. Mlynář[50], D. Molina[8], I. Monakhov[7], M. Moneti[109], R. Mooney[7], S. Moradi[37], S. Mordijck[43], L. Moreira[7], R. Moreno[57], F. Moro[90], A. W. Morris[7], J. Morris[7], L. Moser[26], S. Mosher[73], D. Moulton[7,1], A. Murari[12,35], A. Muraro[45], S. Murphy[7], N. N. Asakura[69], Y. S. Na[80], F. Nabais[53], R. Naish[7], T. Nakano[69], E. Nardon[8], V. Naulin[83], M. F. F. Nave[53], I. Nedzelski[53], G. Nemtsev[88], F. Nespoli[33], A. Neto[41], R. Neu[62], V. S. Neverov[72], M. Newman[7], K. J. Nicholls[7], T. Nicolas[33], A. H. Nielsen[83], P. Nielsen[12], E. Nilsson[8], D. Nishijima[99], C. Noble[7], M. Nocente[97], D. Nodwell[7], K. Nordlund[101], H. Nordman[16], R. Nouailletas[8], I. Nunes[53], M. Oberkofler[62], T. Odupitan[7], M. T. Ogawa[69], T. O'Gorman[7], M. Okabayashi[76], R. Olney[7], O. Omolayo[7], M. O'Mullane[21], J. Ongena[58], F. Orsitto[11], J. Orszagh[18], B. I. Oswuigwe[7], R. Otin[7], A. Owen[7], R. Paccagnella[12], N. Pace[7], D. Pacella[90], L. W. Packer[7], A. Page[7], E. Pajuste[103], S. Palazzo[30], S. Pamela[7], S. Panja[46], P. Papp[18], R. Paprok[50], V. Parail[7], M. Park[66], F. Parra Diaz[27], M. Parsons[73], R. Pasqualotto[12], A. Patel[7], S. Pathak[46], D. Paton[7], H. Patten[33], A. Pau[17], E. Pawelec[48], C. Paz Soldan[43], A. Peackoc[36], I. J. Pearson[7], S.-P. Pehkonen[112], E. Peluso[95], C. Penot[55], A. Pereira[57],

R. Pereira[53], P.P. Pereira Puglia[7], C. Perez von Thun[35,39], S. Peruzzo[12], S. Peschanyi[56], M. Peterka[50], P. Petersson[42], G. Petravich[113], A. Petre[84], N. Petrella[7], V. Petržilka[50], Y. Peysson[8], D. Pfefferlé[33], V. Philipps[39], M. Pillon[90], G. Pintsuk[39], P. Piovesan[12], A. Pires dos Reis[52], L. Piron[7], A. Pironti[105], Pisano[17], R. Pitts[55], F. Pizzo[79], V. Plyusnin[53], N. Pomaro[12], O. G. Pompilian[86], P. J. Pool[7], S. Popovichev[7], M. T. Porfiri[90], C. Porosnicu[86], M. Porton[7], G. Possnert[22], S. Potzel[62], T. Powell[7], J. Pozzi[7], V. Prajapati[46], R. Prakash[46], G. Prestopino[95], D. Price[7], M. Price[7], R. Price[7], P. Prior[7], R. Proudfoot[7], G. Pucella[90], P. Puglia[52], M. E. Puiatti[12], D. Pulley[7], K. Purahoo[7], Th. Pütterich[62], E. Rachlew[25], M. Rack[39], R. Ragona[58], M. S. J. Rainford[7], A. Rakha[6], G. Ramogida[90], S. Ranjan[46], C. J. Rapson[62], J. J. Rasmussen[83], K. Rathod[46], G. Rattá[57], S. Ratynskaia[82], G. Ravera[90], C. Rayner[7], M. Rebai[97], D. Reece[7], A. Reed[7], D. Réfy[113], B. Regan[7], J. Regaña[34], M. Reich[62], N. Reid[7], F. Reimold[39], M. Reinhart[34], M. Reinke[110,73], D. Reiser[39], D. Rendell[7], C. Reux[8], S. D. A. Reyes Cortes[53], S. Reynolds[7], V. Riccardo[7], N. Richardson[7], K. Riddle[7], D. Rigamonti[97], F. G. Rimini[7], J. Risner[73], M. Riva[90], C. Roach[7], R. J. Robins[7], S. A. Robinson[7], T. Robinson[7], D. W. Robson[7], R. Roccella[55], R. Rodionov[88], P. Rodrigues[53], J. Rodriguez[7], V. Rohde[62], F. Romanelli[90], M. Romanelli[7], S. Romanelli[7], J. Romazanov[39], S. Rowe[7], M. Rubel[42], G. Rubinacci[105], G. Rubino[12], L. Ruchko[52], M. Ruiz[94], C. Ruset[86], J. Rzadkiewicz[65], S. Saarelma[7], R. Sabot[8], E. Safi[101], P. Sagar[7], G. Saibene[41], F. Saint-Laurent[8], M. Salewski[83], A. Salmi[112], R. Salmon[7], F. Salzedas[53], D. Samaddar[7], U. Samm[39], D. Sandiford[7], P. Santa[46], M. I. K. Santala[1], B. Santos[53], A. Santucci[90], F. Sartori[41], R. Sartori[41], O. Sauter[33], R. Scannell[7], T. Schlummer[39], K. Schmid[62], V. Schmidt[12], S. Schmuck[7], M. Schneider[8], K. Schöpf[102], D. Schwörer[32], S. D. Scott[76], G. Sergienko[39], M. Sertoli[62], A. Shabbir[15], S. E. Sharapov[7], A. Shaw[7], R. Shaw[7], H. Sheikh[7], A. Shepherd[7], A. Shevelev[54], A. Shumack[38], G. Sias[17], M. Sibbald[7], B. Sieglin[62], S. Silburn[7], A. Silva[53], C. Silva[53], P. A. Simmons[7], J. Simpson[7], J. Simpson-Hutchinson[7], A. Sinha[46], S. K. Sipilä[1], A. C. C. Sips[36], P. Sirén[112], A. Sirinelli[55], H. Sjöstrand[22], M. Skiba[22], R. Skilton[7], K. Slabkowska[49], B. Slade[7], N. Smith[7], P. G. Smith[7], R. Smith[7], T. J. Smith[7], M. Smithies[110], L. Snoj[81], S. Soare[85], E. R. Solano[35,57], A. Somers[32], C. Sommariva[8], P. Sonato[12], A. Sopplesa[12], J. Sousa[53], C. Sozzi[45], S. Spagnolo[12], T. Spelzini[7], F. Spineanu[86], G. Stables[7], I. Stamatelatos[71], M. F. Stamp[7], P. Staniec[7], G. Stankūnas[59], C. Stan-Sion[84], M. J. Stead[7], E. Stefanikova[42], I. Stepanov[58], A. V. Stephen[7], M. Stephen[46], A. Stevens[7], B. D. Stevens[7], J. Strachan[76], P. Strand[16], H. R. Strauss[44], P. Ström[42], G. Stubbs[7], W. Studholme[7], F. Subba[75], H. P. Summers[21], J. Svensson[63], Ł. Świderski[65], T. Szabolics[113], M. Szawlowski[49], G. Szepesi[7], T. T. Suzuki[69], B. Tál[113], T. Tala[112], A. R. Talbot[7], S. Talebzadeh[95], C. Taliercio[12], P. Tamain[8], C. Tame[7], W. Tang[76], M. Tardocchi[45], L. Taroni[12], D. Taylor[7], K. A. Taylor[7], D. Tegnered[16], G. Telesca[15], N. Teplova[54], D. Terranova[12], D. Testa[33], E. Tholerus[42], J. Thomas[7], J. D. Thomas[7], P. Thomas[55], A. Thompson[7], C.-A. Thompson[7], V. K. Thompson[7], L. Thorne[7], A. Thornton[7], A. S. Thrysøe[83], P. A. Tigwell[7], N. Tipton[7], I. Tiseanu[86], H. Tojo[69], M. Tokitani[67], P. Tolias[82], M. Tomeš[50], P. Tonner[7], M. Towndrow[7], P. Trimble[7], M. Tripsky[58], M. Tsalas[38], P. Tsavalas[71], D. Tskhakaya jun[102], I. Turner[7], M. M. Turner[32], M. Turnyanskiy[34], G. Tvalashvili[7], S. G. J. Tyrrell[7], A. Uccello[45], Z. Ul-Abidin[7], J. Uljanovs[1], D. Ulyatt[7], H. Urano[69], I. Uytdenhouwen[78], A. P. Vadgama[7], D. Valcarcel[7], M. Valentinuzzi[8], M. Valisa[12], P. Vallejos Olivares[42], M. Valovic[7], M. Van De Mortel[7], D. Van Eester[58], W. Van Renterghem[78], G. J. van Rooij[38], J. Varje[1], S. Varoutis[56], S. Vartanian[8], K. Vasava[46], T. Vasilopoulou[71], J. Vega[57], G. Verdoolaege[58], R. Verhoeven[7], C. Verona[95], G. Verona Rinati[95], E. Veshchev[55], N. Vianello[45], J. Vicente[53], E. Viezzer[62,92], S. Villari[90], F. Villone[100], P. Vincenzi[12], I. Vinyar[74], B. Viola[90], A. Vitins[103], Z. Vizvary[7], M. Vlad[86], I. Voitsekhovitch[34], P. Vondráček[50], N. Vora[7], T. Vu[8], W. W. Pires de Sa[52], B. Wakeling[7], C. W. F. Waldon[7], N. Walkden[7], M. Walker[7], R. Walker[7], M. Walsh[55], E. Wang[39], N. Wang[39], S. Warder[7], R. J. Warren[7], J. Waterhouse[7], N. W. Watkins[28], C. Watts[55], T. Wauters[58], A. Weckmann[42], J. Weiland[23], H. Weisen[33], M. Weiszflog[22], C. Wellstood[7], A. T. West[7], M. R. Wheatley[7], S. Whetham[7], A. M. Whitehead[7], B. D. Whitehead[7], A. M. Widdowson[7], S. Wiesen[39], J. Wilkinson[7], J. Williams[7], M. Williams[7], A. R. Wilson[7], D. J. Wilson[7], H. R. Wilson[110], J. Wilson[7], M. Wischmeier[62], G. Withenshaw[7], A. Withycombe[7], D. M. Witts[7], D. Wood[7], R. Wood[7], C. Woodley[7], S. Wray[7], J. Wright[7], J. C. Wright[64], J. Wu[89], S. Wukitch[64], A. Wynn[110], T. Xu[7], D. Yadikin[16], W. Yanling[39], L. Yao[89], V. Yavorskij[102], M. G. Yoo[80], C. Young[7], D. Young[7], I. D. Young[7], R. Young[7], J. Zacks[7], R. Zagorski[49], F. S. Zaitsev[18], R. Zanino[75], A. Zarins[103], K. D. Zastrow[7], M. Zerbini[90], W. Zhang[62], Y. Zhou[42], E. Zilli[12], V. Zoita[86], S. Zoletnik[113] and I. Zychor[65]

[1]Aalto University, PO Box 14100, FIN-00076 Aalto, Finland. [2]Aix Marseille Université, CNRS, Centrale Marseille, M2P2 UMR 7340, 13451 Marseille, France. [3]Aix-Marseille Université, CNRS, IUSTI UMR 7343, 13013 Marseille, France. [4]Aix-Marseille Université, CNRS, PIIM, UMR 7345, 13013 Marseille, France. [5]Arizona State University, Tempe, USA. [6]Barcelona Supercomputing Center, Barcelona, Spain. [7]CCFE, Culham Science Centre, Abingdon, Oxon OX14 3DB, UK. [8]CEA, IRFM, F-13108 Saint Paul Lez Durance, France. [9]Center for Energy Research, University of California at San Diego, La Jolla, California 92093, USA. [10]Centro Brasileiro de Pesquisas Fisicas, Rua Xavier Sigaud, 160, Rio de Janeiro CEP 22290-180, Brazil. [11]Consorzio CREATE, Via Claudio 21, 80125 Napoli, Italy. [12]Consorzio RFX, corso Stati Uniti 4, 35127 Padova, Italy. [13]Daegu University, Jillyang, Gyeongsan, Gyeongbuk 712-174, Republic of Korea. [14]Departamento de Física, Universidad Carlos III de Madrid, 28911 Leganés, Madrid, Spain. [15]Department of Applied Physics UG (Ghent University), St-Pietersnieuwstraat 41 B-9000 Ghent, Belgium. [16]Department of Earth and Space Sciences, Chalmers University of Technology, SE-41296 Gothenburg, Sweden. [17]Department of Electrical and Electronic Engineering, University of Cagliari, Piazza d'Armi 09123 Cagliari, Italy. [18]Department of Experimental Physics, Faculty of Mathematics, Physics and Informatics Comenius University Mlynska dolina F2, 84248 Bratislava, Slovak Republic. [19]Department of Materials Science, Warsaw University of Technology, PL-01-152 Warsaw, Poland. [20]Department of Nuclear and Quantum Engineering, KAIST, Daejeon 34141, Korea. [21]Department of Physics and Applied Physics, University of Strathclyde, Glasgow G4 0NG, UK. [22]Department of Physics and Astronomy, Uppsala University, SE-75120 Uppsala, Sweden. [23]Department of Physics, Chalmers University of Technology, SE-41296 Gothenburg, Sweden. [24]Department of Physics, Imperial College London, SW7 2AZ, UK. [25]Department of Physics, SCI, KTH, SE-10691 Stockholm, Sweden. [26]Department of Physics, University of Basel, Switzerland. [27]Department of Physics, University of Oxford, OX1 2JD, UK. [28]Department of Physics, University of Warwick, Coventry, CV4 7AL, UK. [29]Department of Pure and Applied Physics, Queens University, Belfast BT7 1NN, UK.

[30]Dipartimento di Ingegneria Elettrica Elettronica e Informatica-Università degli Studi di Catania, 95125 Catania, Italy. [31]Dipartimento di Ingegneria Industriale, University of Trento, Italy. [32]Dublin City University (DCU), Ireland. [33]Ecole Polytechnique Fédérale de Lausanne (EPFL), Swiss Plasma Center (SPC), CH-1015 Lausanne, Switzerland. [34]EUROfusion Programme Management Unit, Boltzmannstr. 2, 85748 Garching, Germany. [35]EUROfusion Programme Management Unit, Culham Science Centre, Culham OX14 3DB, UK. [36]European Commission, B-1049 Brussels, Belgium. [37]Fluid and Plasma Dynamics, ULB - Campus Plaine - CP 231 Boulevard du Triomphe, 1050 Bruxelles, Belgium. [38]FOM Institute DIFFER, Eindhoven, The Netherlands. [39]Forschungszentrum Jülich GmbH, Institut für Energie- und Klimaforschung - Plasmaphysik, 52425 Jülich, Germany. [40]Fourth State Research, 503 Lockhart Dr, Austin, Texas, USA. [41]Fusion for Energy Joint Undertaking, Josep Pl. 2, Torres Diagonal Litoral B3, 08019 Barcelona, Spain. [42]Fusion Plasma Physics, EES, KTH, SE-10044 Stockholm, Sweden. [43]General Atomics, PO Box 85608, San Diego, California 92186-5608, California, USA. [44]HRS Fusion, West Orange New Jersey, USA. [45]IFP-CNR, via R. Cozzi 53, 20125 Milano, Italy. [46]Institute for Plasma Research, Bhat, Gandhinagar - 382 428 Gujarat, India. [47]Institute of Nuclear Physics, Radzikowskiego 152, 31-342 Kraków, Poland. [48]Institute of Physics, Opole University, Oleska 48, 45-052 Opole, Poland. [49]Institute of Plasma Physics and Laser Microfusion, Hery 23, 01-497 Warsaw, Poland. [50]Institute of Plasma Physics AS CR, Za Slovankou 1782/3, 182 00 Praha 8, Czech Republic. [51]Institute of Plasma Physics, Chinese Academy of Sciences, Hefei 230031, China. [52]Instituto de Física - Universidade de São Paulo Rua do Matão Travessa R Nr.187 CEP 05508- 090 Cidade Universitária, São Paulo, Brasil. [53]Instituto de Plasmas e Fusão Nuclear, Instituto Superior Técnico, Universidade de Lisboa, Portugal. [54]Ioffe Physico-Technical Institute, 26 Politekhnicheskaya, St Petersburg 194021, Russian Federation. [55]ITER Organization, Route de Vinon, CS 90 046, 13067 Saint Paul Lez Durance, France. [56]Karlsruhe Institute of Technology, PO Box 3640, D-76021 Karlsruhe, Germany. [57]Laboratorio Nacional de Fusión, CIEMAT, Madrid, Spain. [58]Laboratory for Plasma Physics Koninklijke Militaire School - Ecole Royale Militaire Renaissancelaan 30 Avenue de la Renaissance B-1000, Brussels, Belgium. [59]Lithuanian energy institute, Breslaujos g. 3, LT-44403 Kaunas, Lithuania. [60]Magnetic Sensor Laboratory, Lviv Polytechnic National University, Lviv, Ukraine. [61]Maritime University of Szczecin, Waly Chrobrego 1-2, 70-500 Szczecin, Poland. [62]Max-Planck-Institut für Plasmaphysik, D-85748 Garching, Germany. [63]Max-Planck-Institut für Plasmaphysik, Teilinsitut Greifswald, D-17491 Greifswald, Germany. [64]MIT Plasma Science and Fusion Centre, Cambridge, Massachusetts 02139, Massachusetts, USA. [65]National Centre for Nuclear Research (NCBJ), 05-400 Otwock-Świerk, Poland. [66]National Fusion Research Institute(NFRI) 169-148 Gwahak-ro, Yuseong-gu, Daejeon 305-806, Republic of Korea. [67]National Institute for Fusion Science, Oroshi, Toki, Gifu 509-5292, Japan. [68]National Institute for Fusion Science, Toki 509-5292, Japan. [69]National Institutes for Quantum and Radiological Science and Technology, Naka, Ibaraki 311- 0193, Japan. [70]National Technical University of Athens, Iroon Politechniou 9, 157 73 Zografou Athens, Greece. [71]NCSR "Demokritos" 153 10, Agia Paraskevi Attikis, Greece. [72]NRC Kurchatov Institute, 1 Kurchatov Square, Moscow 123182, Russian Federation. [73]Oak Ridge National Laboratory, Oak Ridge, Tennessee 37831-6169, Tennessee, USA. [74]PELIN LLC, 27a, Gzhatskaya Ulitsa, Saint Petersburg 195220, Russian Federation. [75]Politecnico di Torino, Corso Duca degli Abruzzi 24, I-10129 Torino, Italy. [76]Princeton Plasma Physics Laboratory, James Forrestal Campus, Princeton, New Jersey 08543, New Jersey, USA. [77]Purdue University, 610 Purdue Mall, West Lafayette, Indiana 47907, USA. [78]SCK-CEN, Nuclear Research Centre, 2400 Mol, Belgium. [79]Second University of Napoli, Consorzio CREATE, Via Claudio 21, 80125 Napoli, Italy. [80]Seoul National University, Shilim-Dong, Gwanak-Gu, Republic of Korea. [81]Slovenian Fusion Association (SFA), Jozef Stefan Institute, Jamova 39, SI-1000 Ljubljana, Slovenia. [82]Space and Plasma Physics, EES, KTH SE-100 44 Stockholm, Sweden. [83]Technical University of Denmark, Department of Physics, Bldg 309, DK-2800 Kgs Lyngby, Denmark. [84]The "Horia Hulubei" National Institute for Physics and Nuclear Engineering, Magurele- Bucharest, Romania. [85]The National Institute for Cryogenics and Isotopic Technology, Ramnicu Valcea, Romania. [86]The National Institute for Laser, Plasma and Radiation Physics, Magurele-Bucharest, Romania. [87]The National Institute for Optoelectronics, Magurele-Bucharest, Romania. [88]Troitsk Insitute of Innovating and Thermonuclear Research (TRINITI), Troitsk 142190, Moscow Region, Russian Federation. [89]Uni of Electronic Science & Tech of China, China. [90]Unità Tecnica Fusione - ENEA C. R. Frascati - via E. Fermi 45, 00044 Frascati (Roma), Italy. [91]Universidad Complutense de Madrid, Madrid, Spain. [92]Universidad de Sevilla, Sevilla, Spain. [93]Universidad Nacional de Educación a Distancia, Madrid, Spain. [94]Universidad Politécnica de Madrid, Grupo I2A2 Madrid, Spain. [95]Università di Roma Tor Vergata, Via del Politecnico 1, Roma, Italy. [96]University College Cork (UCC), Ireland. [97]University Milano-Bicocca, piazza della Scienza 3, 20126 Milano, Italy. [98]University of Basilicata, Consorzio CREATE, Via Claudio 21, 80125 Napoli, Italy. [99]University of California, 1111 Franklin St., Oakland, California 94607, USA. [100]University of Cassino, Consorzio CREATE, Via Claudio 21, 80125 Napoli, Italy. [101]University of Helsinki, PO Box 43, FI-00014 University of Helsinki, Finland. [102]University of Innsbruck, Fusion@Österreichische Akademie der Wissenschaften (ÖAW), Austria. [103]University of Latvia, 19 Raina Blvd., Riga, LV 1586, Latvia. [104]University of Lorraine, CNRS, UMR7198, YIJL, Nancy, France. [105]University of Napoli "Federico II", Consorzio CREATE, Via Claudio 21, 80125 Napoli, Italy. [106]University of Napoli Parthenope, Consorzio CREATE, Via Claudio 21, 80125 Napoli, Italy. [107]University of Texas at Austin, Institute for Fusion Studies, Austin, Texas 78712, Texas, USA. [108]University of Toyama, Toyama 930-8555, Japan. [109]University of Tuscia, DEIM, Via del Paradiso 47, 01100 Viterbo, Italy. [110]University of York, Heslington, York YO10 5DD, UK. [111]Vienna University of Technology, Fusion@Österreichische Akademie der Wissenschaften (ÖAW), Austria. [112]VTT Technical Research Centre of Finland, PO Box 1000, FIN-02044 VTT, Finland. [113]Wigner Research Centre for Physics, PO B. 49, H - 1525 Budapest, Hungary.